

Adversarial Video Promotion Against Text-to-Video Retrieval

Qiwei Tian Chenhao Lin Zhengyu Zhao Shuai Liu Qian Li Chao Shen
Xi'an Jiaotong University
michaeltqw@stu.xjtu.edu.cn, {linchenhao, zhengyu.zhao, qianlix}@xjtu.edu.cn,
{sh_liu, chaoshen}@mail.xjtu.edu.cn

Abstract

Thanks to the development of cross-modal models, text-to-video retrieval (T2VR) is advancing rapidly, but its robustness remains largely unexamined. Existing attacks against T2VR are designed to push videos **away** from queries, i.e., suppressing the ranks of videos, while the attacks that pull videos **towards** selected queries, i.e., promoting the ranks of videos, remain largely unexplored. These attacks can be more impactful as attackers may gain more views/clicks for financial benefits and widespread (mis)information. To this end, we pioneer the first attack against T2VR to promote videos adversarially, dubbed the Video Promotion attack (ViPro). We further propose Modal Refinement (MoRe) to capture the finer-grained, intricate interaction between visual and textual modalities to enhance black-box transferability. Comprehensive experiments cover 2 existing baselines, 3 leading T2VR models, 3 prevailing datasets with over 10k videos, evaluated under 3 scenarios. All experiments are conducted in a multi-target setting to reflect realistic scenarios where attackers seek to promote the video regarding multiple queries simultaneously. We also evaluated our attacks for defences and imperceptibility. Overall, ViPro surpasses other baselines by over 30/10/4% for white/grey/black-box settings on average. Our work highlights an overlooked vulnerability, provides a qualitative analysis on the upper/lower bound of our attacks, and offers insights into potential counterplays. Our manually trained weights are available at <https://github.com/michaeltian108/ViPro>. We will release full code after acceptance.

1. Introduction

Text-to-video retrieval (T2VR) has thrived in recent years, driven by advances in vision-language models (VLM) [11, 23, 37, 44], making it a vital tool for users to search, discover, and consume video content across. While many T2VR models [18, 21, 40, 41] have achieved strong performance on prevailing datasets such as MSR-VTT [43],

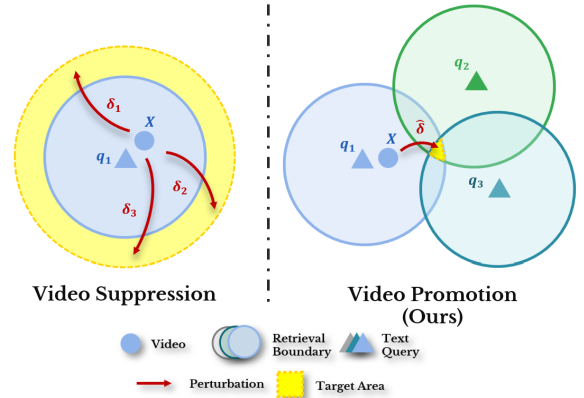


Figure 1. A simplified illustration for video suppression (left) and video promotion (right). The circle represents the retrieval boundary in which videos can be retrieved by the query (text). The yellow shape indicates the targeted area in which the perturbed videos must reach for successful attacks. **Video promotion is more challenging**, as it seeks an intersection of the retrieval boundaries for all target queries, while video suppression only pushes videos outside the retrieval boundary.

DiDeMo [14], and ActivityNet [48], their robustness to adversarial attacks remains largely unexplored. For example, as the only existing attack against T2VR, Yang et al. [45] proposed an adversarial attack against T2VR models to **suppress video ranks** by pushing videos away from queries and vice versa under black-box and white-box settings. However, attacks that **promote videos to top positions** can be more hazardous, as they allow attackers to gain more views/clicks for financial benefits and widespread (mis)information. Additionally, such manipulation can trigger a snowball effect: once the manipulated videos gain initial popularity through adversarial promotion, the platform’s recommendation/retrieval algorithm may further amplify their exposure. Recognizing this overlooked threat, we investigate this vulnerability to video promotion attacks as a critical step towards building robust and trustworthy T2VR systems.

To this end, we propose the first attack against T2VR

to promote videos adversarially for the selected queries, dubbed the Video Promotion attack (ViPro). Furthermore, to reflect realistic user scenarios, we restrict the attack to candidate videos only, without modifying the text queries, as attackers cannot interfere with queries from other users. In Figure. 1, we provide a hypothesized illustration to highlight the difference between existing attacks (video suppression) and ours (video promotion) intuitively. In the left figure, video suppression attacks succeed if the perturbation δ pushes the video \mathbf{X} out of the retrieval boundary of q_1 (depicted as the blue circle), which is determined by the retrieval list length and the videos scattered around the query. Thus, the desired perturbation can be obtained by simply maximizing the distance between the video \mathbf{X} and the query q_1 , as illustrated by the red arrows ($\delta_1, \delta_2, \delta_3$). In contrast, video promotion attacks (right figure) aim to push \mathbf{X} into the small overlapping area (yellow shape) of the retrieval boundaries for all target queries (e.g., q_1, q_2, q_3). Thus, finding the optimal $\hat{\delta}$ requires pre-knowledge of model embeddings and the distribution of target queries.

To overcome the above challenges for better transferability, we propose **Modality Refinement (MoRe)** to guide perturbation towards target areas through finer-grained optimization. MoRe first conducts *Temporal Clipping* to group temporally similar frames into clips, and then applies *Semantic Weighting* to resolve potential gradient conflicts for intra-modality and inter-modality through frame-to-frame and frame-to-query similarities, respectively. Consequently, MoRe provides focused guidance to push the video towards the targeted queries for better transferability. We validate the effectiveness of MoRe through ablation studies in Section.4.3.

Overall, we conduct experiments on 3 open-sourced leading models for MSR-VTT-1k [43], DRL [40], Cap4Video [41], and Singularity [21] (ranked #11/#17/#30¹). We define the white-box, grey-box, and black-box scenarios for ViPro and evaluate its effectiveness and transferability across all three models. For dataset-wise evaluations, we test on **three** prevailing datasets using the Singularity model—ActivityNet [48], DiDeMo [14], and MSR-VTT. As for baselines, we adopt Co-Attack[49] and SGA[29] from the image-to-text domain for comparison, due to the lack of reproducible T2VR-specific attacks. Lastly, we further assess robustness under defences using JPEG compression [10] (image-based) and Temporal Shuffling [16] (video-based). A user study with 17 experts on 43 groups of videos is also conducted for human imperceptibility. **Across all baselines across all datasets, models, and settings, ViPro consistently outperforms other baselines.** Finally, we validate our theoretical motivation through thorough experiments and provide detailed analysis in Section 4.5.

¹Using the leaderboard from paperwithcode.com.

In sum, ViPro exhibits superior effectiveness, generalizability, and transferability over existing baselines, achieving an averaged 30/10/4% lead for white/grey/black-box settings. Our main contributions are listed as follows:

- We introduce a realistic and impactful attacking paradigm for text-to-video retrieval (T2VR) models where attackers promote video ranks for selected queries adversarially. We thus pioneer the Video Promotion Attack (ViPro) as the first attack targeting such vulnerability.
- We propose Modality Refinement (MoRe) to group temporally similar frames into clips and apply semantical weighting using frame-to-frame and frame-to-query similarities for enhanced black-box transferability.
- We conduct thorough experiments and validate the superiority of ViPro over baselines and provide a qualitative analysis of the upper and lower bounds for all attacks.

2. Related Work

Vision-Language Models. Vision-Language models (VLMs), as suggested by the name, require training in both textual and visual encoders. Textual encoders have witnessed the advancement in natural language processing, which progressed from Word2Vec[34] to Bert-base [19, 28] and GPT-based[36] encoders. Besides, visual encoders[1, 6, 7, 9, 24, 30, 39] also advance significantly, surpassing CNN on numerous tasks in the image domain. In light of that, pre-trained VLMs[3, 22, 37, 38, 42, 53] have achieved promising performance on various multi-modal tasks with proper fine-tuning.

Text-to-Video Retrieval. Following the paradigm of VLMs, text-to-video retrieval (T2VR) models also use various off-the-shelf encoders to extract features from videos and their captions[17, 26, 27, 32, 35]. In recent works, CLIP Radford et al. [37] proposes contrastive learning to align visual representations with textual features to achieve an impressive cross-modal retrieval performance. Following this work, many T2VR models have adopted contrastive learning. For example, CLIP-ViP [44] uses pre-trained image-text models and proposes an Omnisource Cross-modal Learning method to contrastively align videos to captions and subtitles. In sum, the architecture of all existing T2VR models can be modelled similarly as “two-plus-one”: two encoders to encode visual and textual inputs, plus one module responsible for cross-modal interaction. All prevailing models can be modelled into such a paradigm, such as Singularity[21] DRL[40], and Cap4Video[41]. Despite the flexibility of such paradigms, the adoption of pre-trained encoders induces risks of adversarial attacks from knowledgeable attackers. Our work shows that ViPro remains effective with the absence of cross-modal modules, even for completely black-box scenarios.

Adversarial attacks on Unimodal Retrieval. Despite numerous explorations on uni-modal and multi-modal re-

trieval [5, 25, 29, 45, 49], existing works largely focus on the untargeted paradigm, i.e., suppressing the ranks of videos regarding their corresponding queries. For example, Li et al. [25] proposed a novel query-based adversarial attack to completely inversed retrieval results for image retrieval. Chen et al. [5] proposed a query-efficient adversarial attack that efficiently suppresses the ranks of manipulated images. Among them, very limited literature has focused on targeted attacks against retrieval models. Specifically, Zhou et al. [52] proposed an Order Attack against image retrieval that manipulates the order of the retrieved results by manipulating the query images.

Adversarial Attacks on Multimodal Retrieval Research on adversarial attacks on multimodal retrieval has primarily focused on the image domain[4, 20, 46, 50, 51]. Recent studies [13, 29, 47, 49] have demonstrated transferable cross-modal adversarial attacks against pre-trained VLM on tasks including text-to-image retrieval, VQA, etc. Yang et al. [45] has proposed an adversarial attack against T2VR models such as Clip4Clip[31], Frozen[2], and BridgeFormer[12]), using the MSR-VTT[43] and DiDeMo[14] datasets. However, this work mainly focused on the untargeted setting to suppress video ranks w.r.t. their corresponding queries.

Another work was conducted by Hu et al. [15]. Specifically, the author proposed a Trojan-horse attack (THA) against text-to-image retrieval that was the first rank promotion adversarial targeted on multiple modalities. Specifically, THA added adversarial QR patches into images to promote the rank of the images w.r.t. target text queries. However, this work only focused on text-to-image retrieval and used an adversarial QR patch as perturbations, which are too obvious and not applicable to videos. Lastly, THA is only targeted at 1 query per image, which is much less challenging than our ViPro, which targets multiple queries simultaneously. Consequently, we raise the importance of investigating targeted attacks against T2VR and propose ViPro as a realistic and impactful attacking paradigm.

3. Methodology

3.1. Threat Model

As illustrated in Table.1, we first define attacking scenarios by categorizing victim models as white-box, grey-box, and black-box. Specifically, the grey-box setting accounts for the situation when the cross-modal interaction module remains unknown to the attackers.

For attackers, we hypothesize that attackers prudently target only semantically relevant queries to avoid obvious misalignment with unrelated queries, e.g., a food video occurs in a sports-related query. Similar to image classification, ViPro can be regarded as a targeted attack focusing on multiple semantically related queries, as we depicted in

Table 1. Settings for attackers’ per-knowledge in different scenarios.

Caption/Category	Attackers’ Pre-knowledge		Attacking
	Unimodal Encoders	Cross-modal Interaction	Scenarios
Caption	✓	✓	White-box
Caption	✓	✗	Grey-box
Category	✗	✗	Black-box

Figure.1.

For queries, we follow existing works[21, 31, 40, 41] and use the paired caption or category of the video as its query. For white-box and grey-box scenarios, attackers can access a subset of queries through the subtitles/descriptions of videos. (See details in Sec.4.1 and the Supplementary.) Specifically, for black-box attacks, attackers can only access the categories (domains) of videos and evaluate the attack accordingly.

Lastly, we formalize the victim model as an open T2VR platform, allowing users to query or upload their videos (e.g., YouTube). Attackers can only launch attacks by uploading manipulated videos to acquire more views/clicks for potential financial gains and widespread (mis)information.

3.2. Video Promotion Attack (ViPro)

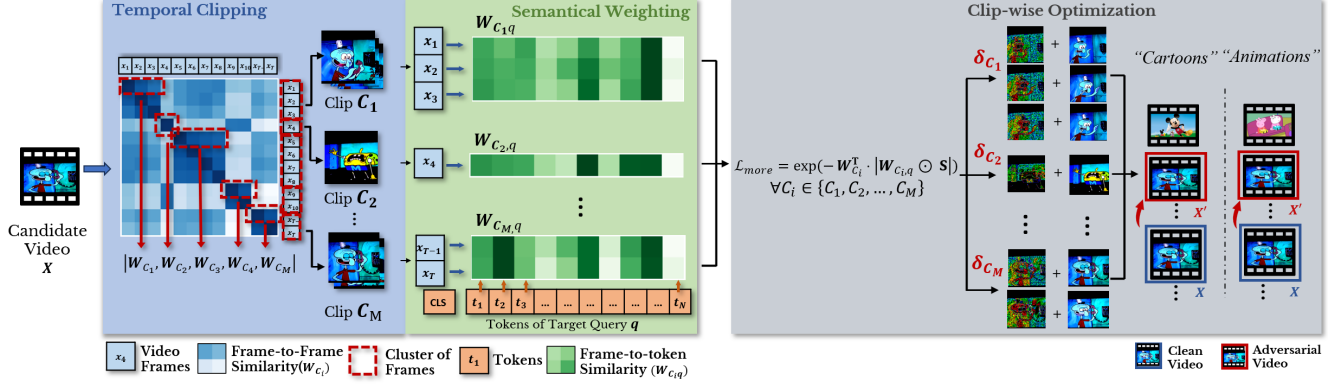
3.2.1. Preliminaries

For a T2VR model, we define \mathcal{V} and \mathcal{T} as the visual and text encoders, respectively, with \mathcal{H} being the cross-modality interaction, which could be a dot product, an MLP layer, or a transformer, etc. Formally, for an input query q , the T2VR task is to rank all videos by their similarities w.r.t. q and output a video list $\mathbb{X}_{q,L}$ that contains the top L relevant video candidates \mathbf{X}_i for the query:

$$\mathcal{H}(\mathcal{T}(q), \mathcal{V}(\mathcal{D})) \rightarrow \mathbf{X}_{q,L} := [\mathbf{X}_1, \mathbf{X}_2, \dots, \mathbf{X}_L]_q \quad (1)$$

The performance of a model can be evaluated based on the number of corresponding videos within the retrieval list $\mathbf{X}_{q,L}$.

Retrieval Boundary. We now formally define the mathematical definition of retrieval boundaries. Based on our hypothesis in Fig.1, for a perturbed video to appear in the retrieval list $\mathbf{X}_{q,L}$, the video must cross the retrieval boundary of the chosen query. Such a boundary is determined by the length of the list L and the spatial distribution of videos in the proximity. We use $L = 1$ to consider top-1 videos only for simplification. Denoting the retrieval boundary of a query q as a hypersphere Φ_q of radius r , r is thus the distance towards its closest video around, denoted \mathbf{X}_q . Once the manipulated video enters Φ_q , the video becomes closer than \mathbf{X}_q , replacing it as the new top-1 video. Thus, the radius of Φ_q , r , is inversely proportional to the similarity of



Modality Refinement (MoRe)

Figure 2. An illustration of our ViPro with MoRe. (1) **Temporal Clipping:** Video frames are clustered into video clips $\mathbb{C} = [C_1, \dots, C_M]$ based on frame-to-frame similarity W_X . (2) **Semantical Weighting:** For each clip and each query, we calculate its frame-to-frame similarity W_{C_i} and frame-to-query similarity $W_{C_i,q}$ using cosine similarity between all frames $x_j \in C_i$ and all query tokens $t_i \in q$. Frames and queries with low similarity are suppressed by their corresponding weights during optimization. (3) **Clip-wise Optimization:** Perturbation are optimized as per clip before outputting the final δ_{C_i} for adversarial video X' .

the closest video nearby. In other words, larger top-1 similarity means smaller r , making it harder for attacks to cross Φ_q , or vice versa.

3.2.2. Attack Objectives

Our goal is to push the candidate video X such that X appears at the top-1 position for all selected queries:

$$X' \in X_{q,L}, \forall q \in Q \quad (2)$$

where $X' := X + \delta$, with δ being the adversarial perturbations. Similar to other adversarial attacks, ViPro also requires visual constraints to keep the attack imperceptible to human eyes, i.e., $\|\delta\|_p \leq \epsilon$, where ϵ is the threshold for the l_p norm. Note that only *visual* modality is attacked.

3.2.3. Loss Function

Due to the discreteness of $X_{q,L}$, Eq.2 is not directly differentiable. We thus apply our retrieval boundary hypothesis above, which translates our objective into pushing X towards the overlap of the retrieval boundaries for all queries in Q , i.e., $X' \in \Phi_{q_1} \cap \Phi_{q_2} \dots \cap \Phi_{q_N}$. The optimal objective to achieve this is to increase the similarity between the candidate video X to exceed the similarity for all top-1 videos $X_q \in X_Q$. However, this optimal objective requires access to X_Q , which is unrealistic. An approximation is to increase the similarity for all queries. Formally, denoting the vision/text feature as F_X and F_q , we define their cross-modality similarity S is defined below:

$$S = \sum_q^Q Sim(F_q, F_X) \quad (3)$$

where $Sim(\cdot)$ refers to the cross-modal interaction to calculate the similarities between videos and queries. For white-box, $Sim(\cdot)$ will be the cross-modal module of victim models, while for grey-box attacks, it will be the cosine similarity. F_X, F_q refer to video and queries features.

A naive solution is to use the negative similarity scores as the loss function directly:

$$\mathcal{L}_{neg}(S) = -S \quad (4)$$

However, \mathcal{L}_{neg} will lead to suboptimal results, especially for multi-target optimization, because it provides identical gradients (i.e., 1) for all targets. Thus, we propose to use exponential loss for optimal results:

$$\mathcal{L}_{exp}(S) = \exp(-S) \quad (5)$$

\mathcal{L}_{exp} could provide adaptive gradients for different targets, i.e., larger gradients for lower S (farther targets) and lower gradients for larger S (nearer targets). Experimental results also validate the effectiveness of \mathcal{L}_{exp} .

3.3. Modality Refinement (MoRe)

An overview of MoRe is presented in Figure 2. For a chosen video $X = [x_1, x_2, \dots, x_T]$ with T frames and the target queries $Q = [q_1, q_2, \dots, q_N]$, MoRe handles the finer-grained interaction between intra-modality and inter-modality in a temporal (intra) and a semantical (inter) respective. Specifically, we first conduct **temporal clipping** to group temporally related frames, and then perform **semantical weighting** to guide optimization using frame-to-token similarity for each query. In this way, MoRe will aid the optimization by guiding it towards target queries for enhanced transferability. Finally, each clip will be optimized separately and concatenated as the manipulated video X' .

Algorithm 1 Pseudo-code for ViPro. **MoRe** will be enabled for generating black-box attacks and disabled otherwise.

Require: Video \mathbf{X} , target queries \mathbf{Q} , visual encoder \mathcal{V} , textual encoder \mathcal{T} , maximum PGD steps K , PGD step size α , perturbation bound ϵ

Ensure: Adversarial Video \mathbf{X}'

```

1: if MoRe then  $\triangleright$  Clip video when MoRe Enabled
2:    $\mathbb{C} = [\mathbf{C}_1, \mathbf{C}_2, \dots, \mathbf{C}_M] \leftarrow \text{TEMPCLIP}(\mathbf{X})$ 
3:   for  $m \leftarrow 1$  to  $M$  do
4:      $\mathbf{C}'_m \leftarrow \text{ATTACK}(\mathbf{C}_m, \mathbf{Q})$   $\triangleright$  Clip-wise Attack
5:   end for
6:    $\mathbf{X}' \leftarrow \text{CONCAT}(\mathbf{C}'_1, \mathbf{C}'_2, \dots, \mathbf{C}'_M)$   $\triangleright$  Concat clips
7: else
8:    $\mathbf{X}' \leftarrow \text{ATTACK}(\mathbf{X}, \mathbf{Q})$ 
9: end if
10: function  $\text{ATTACK}(\mathbb{X}, \mathbf{Q})$   $\triangleright \mathbb{X}$ : input video
11:    $\mathbf{F}_{\mathbb{X}} \leftarrow \mathcal{V}(\mathbb{X}), \mathbf{F}_{\mathbf{Q}} \leftarrow \mathcal{T}(\mathbf{Q})$   $\triangleright$  Get features
12:   if MoRe then  $\triangleright$  Get weights when MoRe enabled
13:      $\mathbf{W}_{\mathbb{X}} \leftarrow \text{COSSIM}(\mathbf{F}_{\mathbb{X}}, \mathbf{F}_{\mathbb{X}})$   $\triangleright$  Frame-to-frame
14:      $\mathbf{W}_{\mathbb{X}, \mathbf{Q}} \leftarrow \text{COSSIM}(\mathbf{F}_{\mathbb{X}}, \mathbf{F}_{\mathbf{Q}})$   $\triangleright$  Frame-to-query
15:   end if
16:   Initialize  $\mathbb{X}'_0 \leftarrow \mathbb{X}, \delta_{\mathbb{X}'_0} \leftarrow 0$ 
17:   for  $k \leftarrow 1$  to  $K$  do
18:      $\mathbb{X}'_k \leftarrow \mathbb{X}'_{k-1} + \delta_{\mathbb{X}'_{k-1}}$ 
19:      $\mathbf{F}_{\mathbb{X}'_k} \leftarrow \mathcal{V}(\mathbb{X}'_k)$ 
20:      $\mathbf{S} \leftarrow \text{Sim}(\mathbf{F}_{\mathbf{Q}}, \mathbf{F}_{\mathbb{X}'_k})$   $\triangleright$  Get sim using Eq.3
21:     if MoRe then  $\triangleright$  Calculate  $\mathcal{L}_{\text{more}}$  using Eq.8
22:        $\mathcal{L} \leftarrow \mathcal{L}_{\text{exp}}(\mathbf{W}_{\mathbb{X}}^T \cdot |\mathbf{W}_{\mathbb{X}, \mathbf{Q}} \odot \mathbf{S}|)$ 
23:     else
24:        $\mathcal{L} \leftarrow \mathcal{L}_{\text{exp}}(\mathbf{S})$   $\triangleright$  Calculate  $\mathcal{L}_{\text{exp}}$  in Eq.5
25:     end if
26:      $\delta_{\mathbb{X}'_{k-1}} \leftarrow \text{PROJ}(\alpha \nabla \mathcal{L}, \epsilon)$   $\triangleright$  PGD
27:   end for
28:   return  $\mathbb{X}'_k$ 
29: end function

```

Temporal Clipping. To accommodate temporal abruptness among video frames (intra-modality), perturbation using averaged gradients from all frames could hinder the convergence of losses and lead to sub-par transferability. An intuitive solution is to perform per-frame optimization, but this would significantly increase computational complexity and break temporal information. Thus, we propose Temporal Clipping to identify temporally outlying frames and group frames into clips. Specifically, for each input video \mathbf{X} , we first calculate its frame-wise cosine similarity $\mathbf{W}_{\mathbf{X}} \in \mathbb{R}^{T \times T}$ as follows:

$$\mathbf{W}_{\mathbf{X}} = \sum \text{CosSim}(x_i, x_i), \forall x_i \in \mathbf{X} \quad (6)$$

We then calculate the similarity difference $\Delta_{\mathbf{W}_{\mathbf{X}}}$ as the temporal shifts between frames, where a larger value indi-

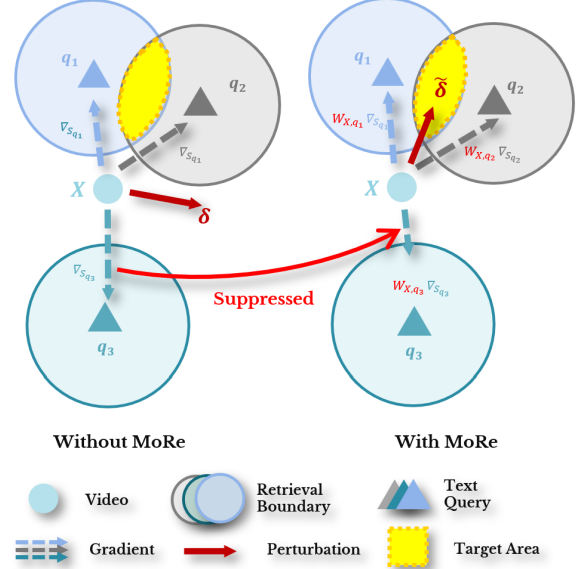


Figure 3. An illustration of the effectiveness of MoRe in guiding optimization. Due to the conflicting gradients, δ in the left figure leads to suboptimal results without entering any boundary. After applying MoRe, the anomalous query (q_3) is suppressed, yielding a more focused perturbation $\tilde{\delta}$ to push videos towards the target area (yellow shape).

cates an outlying frame with palpable temporal abruptness. Subsequently, we loop through all frames and clip them when exceeding the threshold γ . (See detailed pseudo-code in the Supplementary.) Temporal Clipping will output the clipped videos $\mathbb{C} = [\mathbf{C}_1, \dots, \mathbf{C}_M]$ for subsequent clip-to-query alignment.

Semantical Weighting. Similarly, the cross-modality alignment between clips and queries may vary significantly because of the semantic difference. Pushing videos towards them simultaneously may also lead to a ‘looser’ convergence, i.e., failing to enter the retrieval boundary due to conflicting gradient, as shown in the left graph of Figure.3. To avoid this, given a query q and a video clip \mathbf{C} , we calculate the frame-to-query weights $\mathbf{W}_{\mathbf{C}, q}$ using the mean of frame-to-token cosine similarity:

$$\mathbf{W}_{\mathbf{C}, q} = \frac{\sum_j^N \text{CosSim}(x_i, t_j)}{N}, \forall x_i \in \mathbf{C} \quad (7)$$

$\mathbf{W}_{\mathbf{C}, q}$ is subsequently used for weighting the corresponding frames and query for optimal perturbations. In essence, semantic weighting suppresses anomalous queries during optimization to enable a ‘tighter’ convergence towards other queries, as shown in the right graph of Figure.3. The clip-wise temporal similarity $\mathbf{W}_{\mathbf{C}}$ is similarly used as intra-modality semantical weighting to guide frame-level optimization, resolving potential conflicts among gradients from different frames.

Clip-wise Perturbation. Lastly, we optimize the video in a clip-wise manner and present the overall learning objectives of ViPro with MoRe as follows:

$$\mathcal{L}_{more} = \mathcal{L}_{exp} \left(W_{C_i}^T \cdot \left| W_{C_i,q} \odot S \right| \right), \forall C_i \in \mathbb{C} \quad (8)$$

where W_{C_i} , $W_{C_i,q}$, S are all matrices with dimensions of $1 \times T_{C_i}$, $T_{C_i} \times N$ and $T_{C_i} \times N$. T_{C_i} is the number of frames within the clip C_i .

In summary, we incorporate MoRe for a finer-grained alignment of intra-/inter-modalities. Temporal Clipping helps identify and clip temporally outlying frames, while query weighting enables a guided optimization towards target queries by suppressing conflicting gradients. The two modules work cooperatively to push videos further towards target queries for enhanced transferability, which is comprehensively validated through experiments in Section 4.3. Overall, ViPro is used for white-box and grey-box attacks, while MoRe is enabled to generate transferable black-box attacks. We provide a pseudo-code for ViPro and MoRe in Algorithm 1.

4. Experiments

4.1. Experimental Settings

Datasets. We test our attacks on the three prevailing datasets: MSR-VTT-1K (MSR-VTT)[43] contains a 1K testset of YouTube videos, DiDeMo[14] contains a testset of 1065 Flickr videos, and ActivityNet [48] contains a 4.9K testset sampled from YouTube. To ensure equal testset sizes, we randomly sample a 1K subset for all datasets. We use MSR-VTT for model-wise evaluations.

User Queries. As mentioned in Table 1, attackers could access **captions** for white-/grey-box settings and **categories** for the black-box setting. The acquisition of user queries is identical for all scenarios: assuming that all videos come with captions (categories) on T2VR platforms such as YouTube, attackers first use the captions of their own video to query the victim model for the top- K retrieved videos and the corresponding captions (categories). These K captions (categories) are regarded as the relevant queries of this video.

In our experiments, we use $K = 20$ queries and randomly divide them evenly into train/test sets for the hardest scenario where users use different similar but different queries than the ones used for training attacks. *All captions/categories used in our experiments are original from the datasets.* See details of data construction in the Supplementary.

Victim Models. We choose open-sourced leading T2VR models for MSR-VTT on paperwithcode, including Singularity-17M (Sing)[21], DRL-32B (DRL) [40], and Cap4Video-32B (C4V)[41]. DRL and C4V are manually trained on MSR-VTT using the released code. All models

take an input size of $3 \times 224 \times 224$. As for input frames, Sing uses 4 frames per video, while DRL and C4V take 12 frames.

For unimodal encoders, Sing uses BEiT [3] pre-trained on ImageNet-21K [8] for the vision encoder and the first 9 layers of BERT[19] model for the text encoder. DRL and C4V use a Bert-based textual encoder and ViT as its visual encoder. For cross-modal interaction, Sing uses a cross-encoder, and DRL uses a weight-based token interaction for cross-modality interaction. C4V uses a similar token interaction as DRL and introduces a sequence transformer as the video aggregator.

Baselines Due to the lack of directly comparable baselines, we use Co-Attack[49] and SGA[29], which are targeted at text-to-image retrieval (T2IR), as two baselines for comparison. (Attacks introduced by Yang et al. [45] are not included due to the lack of reproducible code.) We then apply the necessary and minimal adaptation to ensure that the two baselines comply with our settings.

For both baselines, textual attacks are not implemented since attackers can only manipulate their updated videos and cannot interfere with user queries. And we reverse the original attacking objectives from **suppressing** ranks to **promoting** ranks. For SGA and ViPro, we use the white-box text-to-video similarities and cosine similarity for white-box and grey-box attacks, respectively. For white-box Co-Attack, we apply its strongest multimodal embedding setting, i.e., minimizing the distance between the perturbed videos and the multimodal embedding of the video-text pairs, denoted as EMB_{Mu1} . For C4V/DRL, which do not feature multimodality embeddings, we modify the objectives to maximize the white-box text-to-video similarity, denoted as SIM_{T2V} . For grey-box Co-attack, we adopt the same cosine similarity for all models.

Evaluation Metrics. We use the difference between vanilla and attacked R@1/5 as evaluation metrics for attacking performance, denoted as $\Delta R@1/5$. Results are presented in the average over the 1K testset for all models/datasets. Higher values are preferable as they indicate efficient attacks.

Hyperparameters. For all attacks, we adopt PGD [33] using l_{inf} norm with $\epsilon = \frac{16}{255}$, $\eta = 2^7$, and the step size $\alpha = 1/255$. Ablation studies for hyperparameters are given in Section 4.3. The random seed is fixed to 42. For the temporal clipping threshold γ , we empirically use $1 - \frac{\sqrt{3}}{2}$ to indicate outlying frames, i.e., frame vectors deviating from the previous one by $\theta \geq \pi/6$.

4.2. Main Results

We first provide white-box results to demonstrate the effectiveness of ViPro as an approximate upper bound. Afterwards, we present grey-box results to show the generalizability of ViPro under restricted knowledge. Finally, we

Table 2. White-box results on all datasets (ActivityNet/DiDeMo/MSR-VTT). The model is Singular. Changes in R@K are presented in the parentheses.

Dataset	Method	R@1(%) ↑	R@5(%) ↑	Average(%) ↑
ActivityNet[48]	-	4.78	24.44	14.61
	Co-Attack[49] (EMB _{Mu1})	3.96 (-0.82)	26.34 (+1.90)	15.15 (+0.54)
	SGA[29]	7.99 (+3.20)	38.44 (+14.00)	23.22 (+8.61)
	ViPro	46.66 (+41.88)	76.25 (+51.81)	61.46 (+46.85)
	ViPro w/o ϵ	76.22 (+71.44)	90.77 (+66.33)	83.50 (+ 68.89)
DiDeMo[14]	-	4.90	24.71	14.78
	Co-Attack[49] (EMB _{Mu1})	5.42 (+0.52)	28.09 (+3.38)	16.76 (+1.95)
	SGA[29]	9.58 (+4.68)	35.08 (+10.37)	22.33 (+7.53)
	ViPro	40.54 (+35.64)	69.56 (+44.85)	55.03 (+40.25)
	ViPro w/o ϵ	66.63 (+61.73)	84.90 (+60.19)	75.74 (+60.96)
MSR-VTT[43]	-	4.87	22.94	13.91
	Co-Attack[49] (EMB _{Mu1})	9.51 (+4.64)	25.12 (+2.18)	17.32 (+3.41)
	SGA[29]	19.30 (+14.43)	46.77 (+23.83)	33.04 (+19.13)
	ViPro	47.81 (+42.94)	73.66 (+50.72)	60.74 (+46.83)
	ViPro w/o ϵ	66.85 (+61.98)	82.53 (+59.59)	74.69 (+60.79)

Table 3. White-box results on all models (Sing/DRL/C4V) using MSR-VTT. Changes in R@K are presented in the parentheses.

Models	Method	R@1(%) ↑	R@5(%) ↑	Average(%) ↑
Sing[21]	No Attack	4.87	22.94	13.91
	Co-Attack[49] (EMB _{Mu1})	9.51 (+4.64)	25.12 (+2.18)	17.32 (+3.41)
	SGA[29]	19.30 (+14.43)	46.77 (+23.83)	33.04 (+19.13)
	ViPro	47.81 (+42.94)	73.66 (+50.72)	60.74 (+46.83)
	ViPro w/o ϵ	66.85 (+61.98)	82.53 (+59.59)	74.69 (+60.79)
DRL[40]	No Attack	4.29	15.76	10.03
	Co-Attack[49] (SIM _{T2V})	61.07 (+56.78)	83.89 (+68.13)	72.48 (+62.46)
	SGA[29]	53.53 (+49.24)	80.37 (+64.61)	66.95 (+56.93)
	ViPro	61.24 (+56.95)	84.62 (+68.86)	72.93 (+62.91)
	ViPro w/o ϵ	87.37 (+83.08)	97.09 (+81.33)	92.23 (+82.21)
C4V[41]	No Attack	3.76	13.42	8.59
	Co-Attack[49] (SIM _{T2V})	75.04 (+71.28)	88.57 (+75.15)	81.81 (+73.22)
	SGA[29]	72.13 (+68.37)	86.99 (+73.57)	79.56 (+70.97)
	ViPro	75.20 (+71.44)	88.91 (+75.49)	82.06 (+73.47)
	ViPro w/o ϵ	93.61 (+89.85)	98.56 (+85.14)	96.09 (+87.50)

conduct cross-model attacks for the transferability of all attacks.

White-Box. We present white-box results on all datasets in Table.2 and all models in Table.3 to demonstrate the effectiveness of ViPro. Overall, all white-box attacks significantly promote video ranks to much higher R@1/5 for all datasets/models, showing the impact of our proposed attacking paradigm across datasets and models. Among them, ViPro achieves the best results over Co-Attack and SGA for all datasets and all models. For dataset-wise comparison, ViPro has a consistent lead for 30% on R@1 over all datasets, especially on ActivityNet, which surpasses Co-Attack and SGA by $\sim 43/38\%$, respectively. ViPro also achieves SOTA performance for model-wise comparison.

For Co-Attack, it constantly performs the worst on all datasets on the Sing model because it applies the KL divergence to optimize using the implicit multimodal embedding to promote videos, which is inefficient in guiding videos towards queries. Once adapted to white-box similarity on DRL and C4V, Co-Attack’s performance benefits signifi-

Table 4. Grey-box results on all datasets (ActivityNet/DiDeMo/MSR-VTT). The model is Sing. Changes in R@K are presented in the parentheses.

Dataset	Method	R@1(%) ↑	R@5(%) ↑	Average(%) ↑
ActivityNet[48]	No Attack	4.78	24.44	14.61
	Co-Attack[49]	4.66 (-0.12)	25.52 (+1.90)	15.09 (+0.48)
	SGA[29]	0.81 (-3.97)	8.24 (-16.20)	4.53 (-10.09)
	ViPro	16.19 (+11.41)	57.84 (+33.40)	37.02 (+22.41)
DiDeMo[14]	No Attack	4.90	24.71	14.78
	Co-Attack[49]	4.48 (-0.42)	22.49 (-2.22)	13.49 (-1.32)
	SGA[29]	1.23 (-3.67)	7.54 (-17.17)	4.39 (-10.42)
	ViPro	8.92 (+4.02)	38.15 (+13.44)	23.51 (+8.73)
MSR-VTT[43]	No Attack	4.87	22.94	13.91
	Co-Attack[49]	4.66 (-0.21)	20.86 (-2.08)	12.76 (-1.15)
	SGA[29]	0.98 (-3.98)	4.05 (-18.89)	2.52 (-11.39)
	ViPro	8.71 (+3.84)	28.9 (+5.85)	18.76 (+4.85)

Table 5. Grey-box results on all models (Sing/DRL/C4V) using MSR-VTT. Changes in R@K are presented in the parentheses.

Models	Method	R@1(%) ↑	R@5(%) ↑	Average(%) ↑
Sing[21]	No Attack	4.87	22.94	13.91
	Co-Attack[49]	4.66 (-0.21)	20.86 (-2.08)	12.76 (-1.15)
	SGA[29]	0.98 (-3.98)	4.05 (-18.89)	2.52 (-11.39)
	ViPro	8.02 (+3.15)	28.31 (+5.37)	18.17 (+4.26)
DRL[40]	No Attack	4.29	15.76	10.03
	Co-Attack[49]	38.61 (+34.328)	76.09 (+60.33)	57.35 (+47.33)
	SGA[29]	39.41 (+35.12)	76.46 (+60.70)	57.97 (+47.91)
	ViPro	42.35 (+38.06)	78.39 (+62.63)	60.37 (+50.35)
C4V[41]	No Attack	3.76	13.42	8.59
	Co-Attack[49]	0.93 (-2.83)	5.07 (-8.35)	3.00 (-5.59)
	SGA[29]	1.28 (-2.48)	7.69 (-5.73)	4.49 (-4.11)
	ViPro	1.99 (-1.77)	10.53 (-2.90)	6.26 (-2.34)

cantly. As for SGA, although it directly utilizes the white-box similarity, it adopts the \mathcal{L}_{neg} defined in Eq.4 plus an aggressive augmentation that includes 4 augmented images. The former leads to suboptimal results since \mathcal{L}_{neg} treats all targets identically, while the latter harms the optimization by augmenting semantically irrelevant videos into training. Specifically, such augmentation could be more damaging on ‘sensitive’ models such as Sing, which is expected to have smaller retrieval boundaries, making it easier for augmented videos to corrupt the semantic correlations between videos and queries. In contrast, DRL and C4V are expected to be less ‘sensitive’ as it has larger retrieval boundaries since SGA shows comparable performance on these models.

Lastly, we present results without perturbation bounds ϵ to demonstrate the experimental upper bound for ViPro attacks to validate our hypothesis on retrieval boundaries. Results on all datasets/models w/o ϵ show that, while gaining certain enhancements, ViPro cannot hit 100% in R@1 and R@5, implying that the distribution of datasets and model embeddings determines the upper bound of ViPro attacks. We will further elaborate on this with an in-depth analysis in Section.4.5.

Grey-Box. We then present the results of all attacks un-

Table 6. Black-Box results of all attacks on MSR-VTT on all models. Results are evaluated using **categories**.

Source	Method	Sing		DRL		C4V		Average(%) \uparrow
Model		R@1(%) \uparrow	R@5(%) \uparrow	R@1(%) \uparrow	R@5(%) \uparrow	R@1(%) \uparrow	R@5(%) \uparrow	
-	No Attack	5.21	9.79	1.42	6.32	0.79	3.00	-
Sing[21]	Co-Attack [49]	-	-	0.63 (-0.79)	5.53 (-0.79)	0.16 (-0.63)	1.74 (-1.26)	2.02 (-0.87)
	SGA [29]	-	-	0.70 (-0.72)	6.00 (-0.32)	0.32 (-0.47)	1.74 (-1.26)	2.19 (-0.69)
	ViPro + MoRe	-	-	1.58 (+0.16)	8.53 (+2.21)	0.32 (-0.47)	3.32 (+0.32)	3.44 (+0.56)
DRL[40]	Co-Attack [49]	7.74 (+2.53)	15.01 (+5.22)	-	-	17.69 (+16.90)	33.33 (+30.33)	18.44 (+13.75)
	SGA [29]	7.58 (+2.37)	15.32 (+5.53)	-	-	22.59 (+21.80)	40.13 (+37.13)	21.41 (+16.71)
	ViPro + MoRe	7.74 (+2.53)	16.11 (+6.32)	-	-	26.05 (+25.26)	45.31 (+42.31)	23.80 (+19.11)
C4V[41]	Co-Attack [49]	5.69 (+0.48)	13.90 (+4.11)	5.21 (+3.79)	20.54 (+14.22)	-	-	11.34 (+5.65)
	SGA [29]	6.95 (+1.74)	13.74 (+3.95)	7.11 (+5.69)	23.70 (+17.38)	-	-	12.88 (+7.19)
	ViPro + MoRe	7.63 (+2.42)	13.99 (+4.20)	26.05 (+24.63)	46.31 (+39.99)	-	-	23.50 (+17.81)

der the grey-box setting for all datasets/models. In Table.4 and Table.5, SGA and Co-attack fail to promote the R@1 of perturbed videos for most cases, incurring negative promotion after attacks. In contrast, our ViPro manages to generalize well and retain its advantages over other baselines for all datasets. For example, on DiDeMo and MSR-VTT, our ViPro is the only method that successfully promotes manipulated video, while other baselines are shown to be inefficient for grey-box attacks. For model-wise comparison, ViPro also achieves the SOTA results for all models. Specifically, SGA experienced large performance drops on all datasets, echoing our conclusion on the damage brought by augmentation on ‘sensitive’ models. These leads further validate the effectiveness of our proposed ViPro over SGA and Co-Attack for promoting videos.

Compared to white-box settings, all grey-box attacks experience a performance downgrade. Specifically, we observe inconsistency in performance drops compared to their white-box counterparts. For example, attacks on DRL experienced the minimum degradations by only 15/9/12% for Co-Attack/SGA/ViPro, respectively. On the other hand, attacks on C4V decrease significantly by over 60% on average for all attacks, which is caused by the introduction of an extra video aggregator. We provide an ablation to validate this in the Supplementary, where all attacks show significant performance boosts with access to the aggregator. We will discuss these findings in Section. 4.5.

Black-Box. We finally evaluate cross-model transferability in the black-box settings following the definition in Table.1, where attackers can only access the categorical information from the video. Thus, black-box attackers could only target the annotated category to promote its rank under this category. We use the categories provided in the original paper in [43]. Specifically, we use the 10 out of 20 categories with the best zero-shot R-Precision on all models. Details on evaluations for all models and categories are provided in the Supplementary.

Results are given in Table.6. Overall, ViPro retains its

lead over all baselines for all black-box models, leading Co-Attack and SGA by 6% and 4% on average. Specifically, when using C4V as the source model, ViPro significantly outperforms Co-Attack and SGA by 21/26% and 19/23% for R@1/5 when attacking DRL models. ViPro also surpasses the other two baselines by 5% and 2% on DRL-generated attacks, yielding a maximum 25.26% promotion on R@1 and 42.31% on R@5 when attacking C4V. As for the attacks optimized using Sing, our ViPro is the only method that achieves improved overall average R@1/5 among all methods, yielding a 0.5% promotion over Co-Attack (-0.87%) and SGA (-0.69%). The results validate the advantages of ViPro + MoRe for transferability.

Besides, comparing attacks generated by different models, we find that attacks from Sing exhibit the least transferability than those generated by DRL and C4V, while DRL and C4V show better transferability to the others. This observation aligns with the consensus that models exhibit better/worse transferability on similar/dissimilar models: C4V and DRL models adopt the same ViT encoders, while Sing uses BEiT.

4.3. Ablation Study

In this section, we first demonstrate the effectiveness of MoRe in improving transferability, with a specific comparison between temporal clipping and random clipping. Afterwards, we conduct a qualitative evaluation on the impact of the number of training targets on optimizing ViPro, yielding counter-intuitive yet inspiring results. We finally provide an ablation study on the hyperparameters used in PGD.

Modality Refinement. To validate the viability of Temporal Clipping, we provide results without MoRe and MoRe with random clipping (denoted as MoRe \mathcal{R}) for comparison. Results are presented as the average results of each source model for clarity, as shown in Table.7. First of all, we observe sub-par or the worst performance for the random clipping, i.e., MoRe \mathcal{R} . For example, on the Sing model, random clipping leads to downgraded performance

Table 7. Ablation studies on the effectiveness of MoRe to boost transferability. \mathcal{R} denotes random clipping. Results are given as the average of each source model. MoRe achieves the **best overall black-box performances for ALL models**.

Source Model	Method	R@1(%) \uparrow	R@5(%) \uparrow	Average (%) \uparrow
Sing[21]	ViPro	0.87(-0.24)	5.92 (+1.26)	3.39 (+0.51)
	ViPro + MoRe \mathcal{R}	0.79 (-0.32)	5.37 (+0.71)	3.08 (+0.20)
	ViPro + MoRe	0.95 (-0.16)	5.93 (+1.27)	3.44 (+0.56)
DRL[40]	ViPro	14.06 (+11.06)	27.25 (+20.86)	20.66 (+15.96)
	ViPro + MoRe \mathcal{R}	15.49 (+12.49)	27.57 (+21.17)	21.53 (+16.83)
	ViPro + MoRe	16.90 (+13.90)	30.71(+24.32)	23.80 (+19.11)
C4V[41]	ViPro	15.33 (+12.01)	25.68 (+17.62)	20.50 (+14.82)
	ViPro + MoRe \mathcal{R}	12.00 (+8.69)	26.74 (+18.60)	19.37 (+13.69)
	ViPro + MoRe	16.84 (+13.53)	30.15 (+22.10)	23.50 (+17.81)

for both R@1 and R@5, yielding the worst results for the model. Moreover, the R@1 also drops significantly by over 3% on attacks generated by C4V, implying that randomly clipping the video would potentially incur worse attacking performance. On the other hand, our ViPro + MoRe consistently achieves the best performance over its counterparts with random clipping and ViPro itself across models. For example, our MoRe brings a 2.9/3% boost over ViPro on DRL regarding R@1/5, and a 1.5/5% boost on C4V regarding R@1/5. For the most challenging source model, our ViPro + MoRe also boosts the R@1/5 considerably. This validates the effectiveness of our MoRe to ‘tighten’ the convergence of losses during the optimization of perturbations by clustering temporally similar frames and guiding optimization with query weighting.

Number of Training Queries. Intuitively, the number of training queries for optimizing ViPro could significantly influence attack performance. Intuition may be that ViPro would benefit from larger numbers of training queries as it acquires more knowledge about the victim datasets. To this end, we trial different numbers of training queries on all datasets and models, ranging from 10 (experiment setting) to 500 (half of the testset).

As shown in Figure 4, we find counter-intuitive results as the number of training queries increase for both white- & grey-box attacks: for dataset-wise comparison (top row), the attacking performance suffers from a constant drop, yielding an over 40% degradation as the number reaches 500; for model-wise comparison (bottom row), the results on DRL and C4V exhibits a rise-to-plateau trend, with a minor drop in the late stage. Specifically, for DRL and C4V, using only 10 training queries can efficiently achieve more than 85% of the max performance when using more queries, whereas for Sing, using 10 already achieves the best results over others. Overall, we can draw the following conclusion: Using more queries does not necessarily boost attacking performance, while **a small number of queries is sufficient to generate effective attacks for both white-box and grey-box ViPro**.

Hyperparameters. Ablations on PGD hyperparameters on

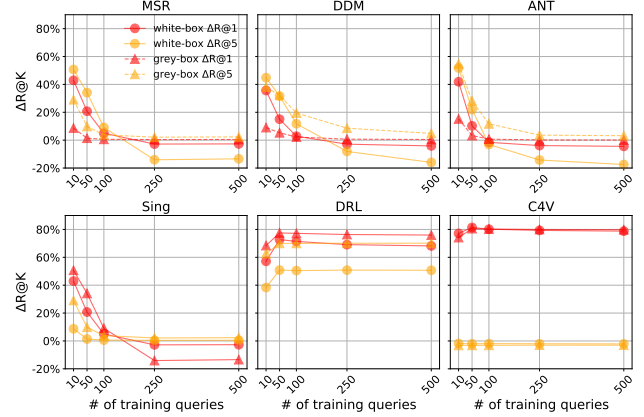


Figure 4. The impact of varying numbers of training queries for white-box (solid lines) and grey-box (dashed lines) ViPro on all datasets (top row) and all models (bottom row). We present $\Delta R@1$ (red) and $\Delta R@5$ (orange).

all datasets are presented in Figure 5, showing the results for max steps η , step size α , and perturbation bound ϵ . We use white-box results on the Sing model for all datasets and present R@1 changes to demonstrate attacking performance.

For the max PGD step size η , we observe a monotonic increase as it increases from 2^4 to 2^9 for all datasets. Considering the computational cost of perturbing videos, we choose 2^7 for balanced results between effectiveness and efficiency. Although further increasing η would boost attacking performance, such boosts come at the cost of doubled or more training time. For the step size α , we test values ranging from 1 to 4. Consistent with our previous speculation, ViPro suffers from a steady performance drop as the step sizes increase. This echoes with our illustration in Fig. 1 that video promotion is an intricate attack that requires sophisticated optimization for optimal results. Finally, a similar trend as η is found for the perturbation budget ϵ . Thus, we empirically choose $\epsilon = 16$ for better effectiveness while maintaining imperceptibility. We also use a user study to examine the stealthiness of our ViPro over Co-Attack and SGA under the same ϵ in Sec. 4.4.

4.4. Evaluation under Realistic Scenarios

In reality, attacks against T2VR may undergo defenses such as JPEG compression during upload. Besides, it is also vital that manipulated videos do not contain artifacts or visual clues that are obvious to human users. Consequently, to comprehensively evaluate the performance of all attacks under realistic scenarios, we perform evaluations for all attacks regarding both robustness against defences and human evaluations.

Robustness against Defences. To verify the robustness of all attacks under defence, we adopt JPEG Compression (JC)

Table 8. White-box defense evaluations using Temporal Shuffling and JPEG Compression on Sing, DRL, and C4V. Changes after attacks are presented in parentheses. **Our ViPro retains its superiority under both defences.**

Defense	Attack	Sing		DRL		C4V		Average(%) \uparrow
		R@1(%) \uparrow	R@5(%) \uparrow	R@1(%) \uparrow	R@5(%) \uparrow	R@1(%) \uparrow	R@5(%) \uparrow	
-	No Attack	4.87	22.94	4.29	15.76	3.79	13.73	-
Temporal Shuffling[16]	Co-Attack [49]	8.33 (+3.46)	21.48(-1.46)	38.82 (+34.53)	62.95 (+47.19)	55.74 (+51.95)	73.58 (+59.85)	43.48 (+32.59)
	SGA [29]	17.11 (+12.24)	41.83 (+18.89)	36.05 (+31.76)	60.42 (+44.66)	53.20 (+49.41)	71.24 (+57.51)	46.64 (+35.75)
	ViPro	38.39 (+33.52)	64.67 (+41.73)	39.32 (+35.03)	63.95 (+48.19)	55.51 (+51.72)	73.28 (+59.55)	55.85 (+44.96)
JPEG Compression[10] ($q = 75$)	Co-Attack [49]	8.49 (+3.62)	23.18(+0.24)	53.46 (+49.17)	77.55 (+61.79)	67.55 (+63.76)	84.24 (+70.51)	52.41 (+41.52)
	SGA [29]	19.21 (+14.34)	46.59 (+23.65)	52.93 (+48.64)	77.80 (+62.04)	67.82 (+64.03)	84.20 (+70.47)	58.09 (+47.20)
	ViPro	34.85 (+29.98)	63.67 (+40.73)	53.57 (+49.28)	78.00 (+62.24)	67.76 (+66.97)	84.26 (+70.53)	63.69 (+52.79)

Table 9. Grey-Box defense evaluations using Temporal Shuffling and JPEG Compression on Sing, DRL, and C4V. Changes after attacks are presented in parentheses. **Our ViPro retains its superiority under both defences.**

Defense	Attack	Sing		DRL		C4V		Average(%) \uparrow
		R@1(%) \uparrow	R@5(%) \uparrow	R@1(%) \uparrow	R@5(%) \uparrow	R@1(%) \uparrow	R@5(%) \uparrow	
-	No Attack	4.87	22.94	4.29	15.76	3.79	13.73	-
Temporal Shuffling[16]	Co-Attack [49]	4.65 (-0.22)	19.88 (-3.06)	21.08 (+16.79)	53.31 (+37.55)	0.47 (-3.32)	3.73 (-10.00)	17.19 (+6.29)
	SGA [29]	0.89 (-3.98)	3.93 (-19.01)	24.56 (+20.27)	60.58 (+44.82)	1.19 (-2.60)	7.32 (-6.41)	16.41 (+5.52)
	ViPro	8.44 (+3.57)	27.44 (+4.50)	37.84 (+33.55)	72.09 (+56.33)	1.83 (-1.96)	10.15 (-3.58)	26.30 (+15.40)
JPEG Compression[10] ($q = 75$)	Co-Attack [49]	5.06 (+0.19)	20.53(-2.41)	30.94 (+26.65)	67.22 (+51.46)	0.22 (-3.57)	1.92 (-11.81)	20.98 (+10.09)
	SGA [29]	1.14 (-3.73)	4.52 (-18.42)	36.51 (+32.22)	73.45 (+57.69)	1.27 (-2.52)	6.91 (-6.82)	20.63 (+9.74)
	ViPro	7.80 (+2.93)	28.26 (+5.32)	46.26 (+41.97)	79.79 (+64.03)	1.57 (-2.22)	8.37 (-5.36)	28.68 (+17.78)

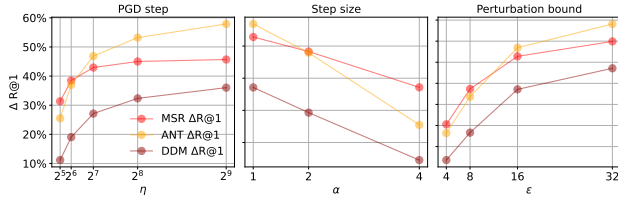


Figure 5. Ablation studies on PGD hyperparameters, showing results for max PGD steps η , step size α , and perturbation bound ϵ , respectively. Results are presented in R@1 changes after attacks, denoted as $\Delta R@1$. R@5 results are not presented for better visibility.

[10] and Temporal Shuffling (TS) [16], two well-recognized image-based and video-based defences, to evaluate all included attacks on all models for white-box and grey-box scenarios. Following the settings in the original papers, we use JPEG with $q = 75$, and for TS, we use $h_1 = 2, h_2 = 1$ for Sing (uses 4 frames), and $h_1 = 4, h_2 = 2$ for DRL and C4V (use 12 frames). Results are presented in Table.8 and Table.9. Our ViPro shows the best overall robustness against both image-based and video-based defences, leading to Co-Attack by 10/9% and SGA by 7/9% for white-/grey-box settings, respectively.

Imperceptibility for Human. We finally provide evaluations on the visual imperceptibility of all attacks. We first present a visualization of all attacks in Fig. 6, from which we find SGA as the most suspicious compared to Co-Attack

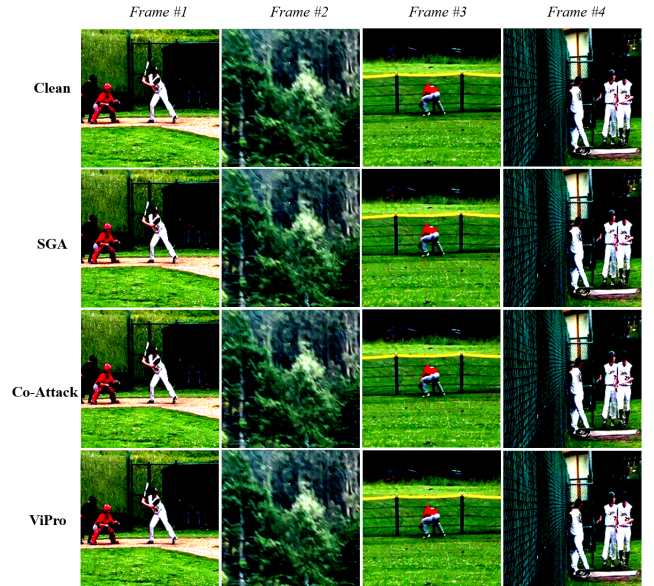


Figure 6. Visualization of original frames and manipulated frames for all attacks (white-box). From top to bottom: **Clean**, **SGA**, **Co-Attack**, **ViPro (ours)**. SGA has the most obvious patterns and artifacts. Co-Attack has on-par stealthiness as our ViPro with minor visual clues, while **our ViPro remains stealthy with the best performance.**

and ViPro. We attribute this to its more aggressive data augmentation strategy that leads to diverse but perceptible

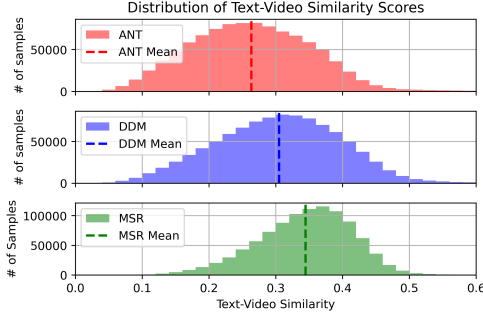


Figure 7. Visualization of white-box top 1 text-to-video similarity scores for all datasets. All results are normalized between 0 to 1 for better visibility.

perturbations. We further conducted a user study with 43 shuffled groups of videos for each attack. Based on results from 17 human experts (i.e., equipped with background knowledge about adversarial attacks), ViPro is chosen as the stealthiest with **42.69%** of cases, beating both Co-Attack **39.47%** and SGA **17.84%**, proving ViPro’s stealthiness.

4.5. Discussion

In this section, we will elaborate on the mechanism behind the ViPro attack, including a qualitative analysis on the determinants for **upper bound** and the **lower bound** of video promotion attacks. We then investigate the potential defensive practices against ViPro attacks. Finally, we discuss the limitations and future works of our paper.

Upper Bound. The upper bound refers to the theoretically achievable maxima on a victim model for all attacks, which is jointly determined by *the distribution of model embeddings* and *the distribution of the dataset*. The results w/o ϵ across datasets and models in Table.2 and Table.3 can also support the previous conclusion. For example, ActivityNet has the highest R@1 and R@5 than MSR-VTT and DiDeMo, while the results on Sing show the lowest R@1/5 over DRL and C4V. Following our previous theory on retrieval region, ActivityNet is supposed to have the largest retrieval region for all datasets, while Sing has the tightest (smallest) region for all models. This translates to the smallest average text-video similarities for ActivityNet and the largest ones for Sing. To validate this, we plot histograms of text-video similarities for all datasets and models. As shown in Figure.7 and Figure.8, the distribution and mean of the similarities for all datasets and models align with our previous speculation. The results also echo our previous speculation on model ‘sensitivity’: With the largest average top-1 similarity, Sing is the most sensitive model to variation in the embedding, making SGA the least effective attack due to augmentation, and vice versa for C4V and DRL. This verifies our theory on the two determinants: the model

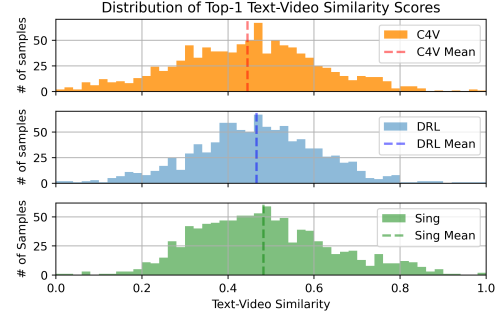


Figure 8. Visualization of white-box top 1 text-to-video similarity scores for all models. Because the embeddings vary significantly across models, we only present normalized top 1 scores for better visibility.

distribution of model embeddings and the dataset.

Lower Bound. The lower bound refers to the generalization ability of attacks to maintain their effectiveness across settings. We hypothesize the algorithms of attacks and the architecture of victim models as the two determining factors. For algorithms, we show in the main results and ablation studies that ViPro consistently outperforms its counterparts using KL divergence (Co-Attack) and naive negative loss (SGA). Besides, the incorporation of MoRe also implies that the explicit design in refining temporal and semantical interaction further improves the ability to generalize across models. As for model architecture, we find that models with a structural cross-modal interaction exhibit stronger resistance to non white-box attacks. For example, as shown in Table.5, DRL experiences the least performance drop compared to white-box results, given that it is the only model using algorithmic cross-modal interaction. C4V, in contrast, shows the strongest resistance because of its video aggregator within the cross-modal module. Furthermore, according to our ablation study in the Supplementary, the inclusion of access to the video aggregator would significantly boost all attacks compared to grey-box settings. These findings shed light on possible ways in building robust T2VR models, especially when using open-sourced pre-trained encoders.

Potential Defense against ViPro. As presented in Table.8 and Table.9, ViPro remains effective under popular image and video defences. To better protect T2VR models from such attacks, popular methods such as adversarial fine-tuning and purification could also be an efficient protection. However, the former may cause large performance degradation, while the latter requires computational optimization for faster video purification. Thus, we suggest using more information-rich modalities, such as audio, for multimodal fusion. From our observation for the attack lower bound, the inclusion of encoders for more modalities

would increase the robustness of models and weaken the dependence of models on visual information.

Limitations & Future Work. Due to the computational overhead, we cannot test our attacks on larger VLMs but use deployable open-sourced models for evaluations. Thus, we cannot launch effective attacks on larger commercial T2VR platforms such as YouTube. Besides, the transferability can be further boosted using more accurate temporal clipping, i.e., model-aided clustering, and/or model ensemble. Lastly, temporal constraints can also be applied for better stealthiness of manipulated videos to avoid visual clues and artifacts. These directions are valuable for future exploration.

5. Conclusion

We explore the overlooked vulnerability against text-to-video retrieval (T2VR) and propose a new attacking paradigm to promote video ranks adversarially. Accordingly, we pioneer the Video Promotion attack (ViPro) as the first attack targeting such vulnerability. We further propose Modality Refinement (MoRe) to capture the intricate modality interaction to enhance black-box transferability. Comprehensive experiments include 2 existing baselines, 3 leading T2VR models, 3 prevailing datasets with over 10k videos, evaluated under 3 scenarios. All experiments are conducted in a multi-target setting to reflect realistic scenarios where attackers seek to promote the video regarding multiple queries simultaneously. We also provide evaluations for defences and imperceptibility. In sum, ViPro consistently shows the best performance on all settings over existing baselines, implying the superiority of our method. Our work provides a qualitative analysis on the upper and lower bounds of ViPro, highlights an overlooked vulnerability, and offers insights into potential counterplays.

References

- [1] Peter Anderson, Xiaodong He, Chris Buehler, Damien Teney, Mark Johnson, Stephen Gould, and Lei Zhang. Bottom-up and top-down attention for image captioning and visual question answering. In *Proceedings of the IEEE conference on computer vision and pattern recognition*, pages 6077–6086, 2018. 2
- [2] Max Bain, Arsha Nagrani, Gül Varol, and Andrew Zisserman. Frozen in time: A joint video and image encoder for end-to-end retrieval, 2022. 3
- [3] Hangbo Bao, Li Dong, Songhao Piao, and Furu Wei. Beit: Bert pre-training of image transformers. *arXiv preprint arXiv:2106.08254*, 2021. 2, 6
- [4] Hongge Chen, Huan Zhang, Pin-Yu Chen, Jinfeng Yi, and Cho-Jui Hsieh. Show-and-fool: Crafting adversarial examples for neural image captioning. *arXiv preprint arXiv:1712.02051*, 2, 2017. 3
- [5] Mingyang Chen, Junda Lu, Yi Wang, Jianbin Qin, and Wei Wang. Dair: A query-efficient decision-based attack on image retrieval systems. In *Proceedings of the 44th International ACM SIGIR Conference on Research and Development in Information Retrieval*, pages 1064–1073, 2021. 3
- [6] Yen-Chun Chen, Linjie Li, Licheng Yu, Ahmed El Kholy, Faisal Ahmed, Zhe Gan, Yu Cheng, and Jingjing Liu. Uniter: Learning universal image-text representations. 2019. 2
- [7] Yen-Chun Chen, Linjie Li, Licheng Yu, Ahmed El Kholy, Faisal Ahmed, Zhe Gan, Yu Cheng, and Jingjing Liu. Uniter: Learning universal image-text representations. 2019. 2
- [8] Jia Deng, Wei Dong, Richard Socher, Li-Jia Li, Kai Li, and Li Fei-Fei. Imagenet: A large-scale hierarchical image database. In *2009 IEEE conference on computer vision and pattern recognition*, pages 248–255. Ieee, 2009. 6
- [9] Alexey Dosovitskiy, Lucas Beyer, Alexander Kolesnikov, Dirk Weissenborn, Xiaohua Zhai, Thomas Unterthiner, Mostafa Dehghani, Matthias Minderer, Georg Heigold, Sylvain Gelly, et al. An image is worth 16x16 words: Transformers for image recognition at scale. *arXiv preprint arXiv:2010.11929*, 2020. 2
- [10] Gintare Karolina Dziugaite, Zoubin Ghahramani, and Daniel M. Roy. A study of the effect of jpg compression on adversarial images, 2016. 2, 10
- [11] Zijian Gao, Jingyu Liu, Sheng Chen, Dedan Chang, Hao Zhang, and Jinwei Yuan. Clip2tv: An empirical study on transformer-based methods for video-text retrieval. *arXiv preprint arXiv:2111.05610*, 1(2):6, 2021. 1
- [12] Yuying Ge, Yixiao Ge, Xihui Liu, Dian Li, Ying Shan, Xiaohu Qie, and Ping Luo. Bridging video-text retrieval with multiple choice questions, 2022. 3
- [13] Bangyan He, Xiaojun Jia, Siyuan Liang, Tianrui Lou, Yang Liu, and Xiaochun Cao. Sa-attack: Improving adversarial transferability of vision-language pre-training models via self-augmentation, 2023. 3
- [14] Lisa Anne Hendricks, Oliver Wang, Eli Shechtman, Josef Sivic, Trevor Darrell, and Bryan Russell. Localizing moments in video with natural language. In *Proceedings of the IEEE International Conference on Computer Vision (ICCV)*, 2017. 1, 2, 3, 6, 7
- [15] Fan Hu, Aozhu Chen, and Xirong Li. Towards making a trojan-horse attack on text-to-image retrieval. In *ICASSP 2023-2023 IEEE International Conference on Acoustics, Speech and Signal Processing (ICASSP)*, pages 1–5. IEEE, 2023. 3
- [16] Jaehui Hwang, Huan Zhang, Jun-Ho Choi, Cho-Jui Hsieh, and Jong-Seok Lee. Temporal shuffling for defending deep action recognition models against adversarial attacks. *Neural Networks*, 169:388–397, 2024. 2, 10
- [17] Peng Jin, Jinfa Huang, Fenglin Liu, Xian Wu, Shen Ge, Guoli Song, David Clifton, and Jie Chen. Expectation-maximization contrastive learning for compact video-and-language representations. *Advances in Neural Information Processing Systems*, 35:30291–30306, 2022. 2
- [18] Peng Jin, Jinfa Huang, Pengfei Xiong, Shangxuan Tian, Chang Liu, Xiangyang Ji, Li Yuan, and Jie Chen. Video-text as game players: Hierarchical banzhaf interaction for cross-modal representation learning. In *Proceedings of the IEEE/CVF Conference on Computer Vision and Pattern Recognition*, pages 2472–2482, 2023. 1

- [19] Jacob Devlin Ming-Wei Chang Kenton and Lee Kristina Toutanova. Bert: Pre-training of deep bidirectional transformers for language understanding. In *Proceedings of naacL-HLT*, page 2, 2019. 2, 6
- [20] Raz Lapid and Moshe Sipper. I see dead people: Gray-box adversarial attack on image-to-text models, 2023. 3
- [21] Jie Lei, Tamara Berg, and Mohit Bansal. Revealing single frame bias for video-and-language learning. In *Proceedings of the 61st Annual Meeting of the Association for Computational Linguistics (Volume 1: Long Papers)*, pages 487–507, Toronto, Canada, 2023. Association for Computational Linguistics. 1, 2, 3, 6, 7, 8, 9
- [22] Junnan Li, Ramprasaath R. Selvaraju, Akhilesh Deepak Gotmare, Shafiq Joty, Caiming Xiong, and Steven Hoi. Align before fuse: Vision and language representation learning with momentum distillation, 2021. 2
- [23] Junnan Li, Dongxu Li, Caiming Xiong, and Steven Hoi. BLIP: Bootstrapping language-image pre-training for unified vision-language understanding and generation. In *Proceedings of the 39th International Conference on Machine Learning*, pages 12888–12900. PMLR, 2022. 1
- [24] Xiujun Li, Xi Yin, Chunyuan Li, Pengchuan Zhang, Xiaowei Hu, Lei Zhang, Lijuan Wang, Houdong Hu, Li Dong, Furu Wei, et al. Oscar: Object-semantics aligned pre-training for vision-language tasks. In *Computer Vision—ECCV 2020: 16th European Conference, Glasgow, UK, August 23–28, 2020, Proceedings, Part XXX 16*, pages 121–137. Springer, 2020. 2
- [25] Xiaodan Li, Jinfeng Li, Yuefeng Chen, Shaokai Ye, Yuan He, Shuhui Wang, Hang Su, and Hui Xue. Qair: Practical query-efficient black-box attacks for image retrieval. In *Proceedings of the IEEE/CVF Conference on Computer Vision and Pattern Recognition*, pages 3330–3339, 2021. 3
- [26] Yang Liu, Samuel Albanie, Arsha Nagrani, and Andrew Zisserman. Use what you have: Video retrieval using representations from collaborative experts. *arXiv preprint arXiv:1907.13487*, 2019. 2
- [27] Yang Liu, Samuel Albanie, Arsha Nagrani, and Andrew Zisserman. Use what you have: Video retrieval using representations from collaborative experts. *arXiv preprint arXiv:1907.13487*, 2019. 2
- [28] Yinhan Liu, Myle Ott, Naman Goyal, Jingfei Du, Mandar Joshi, Danqi Chen, Omer Levy, Mike Lewis, Luke Zettlemoyer, and Veselin Stoyanov. Roberta: A robustly optimized bert pretraining approach. *arXiv preprint arXiv:1907.11692*, 2019. 2
- [29] Dong Lu, Zhiqiang Wang, Teng Wang, Weili Guan, Hongchang Gao, and Feng Zheng. Set-level guidance attack: Boosting adversarial transferability of vision-language pre-training models. In *Proceedings of the IEEE/CVF International Conference on Computer Vision (ICCV)*, pages 102–111, 2023. 2, 3, 6, 7, 8, 10
- [30] Jiasen Lu, Dhruv Batra, Devi Parikh, and Stefan Lee. Vilbert: Pretraining task-agnostic visiolinguistic representations for vision-and-language tasks. *Advances in neural information processing systems*, 32, 2019. 2
- [31] Huaishao Luo, Lei Ji, Ming Zhong, Yang Chen, Wen Lei, Nan Duan, and Tianrui Li. Clip4clip: An empirical study of clip for end to end video clip retrieval, 2021. 3
- [32] Huaishao Luo, Lei Ji, Ming Zhong, Yang Chen, Wen Lei, Nan Duan, and Tianrui Li. Clip4clip: An empirical study of clip for end to end video clip retrieval and captioning. *Neurocomputing*, 508:293–304, 2022. 2
- [33] Aleksander Madry, Aleksandar Makelov, Ludwig Schmidt, Dimitris Tsipras, and Adrian Vladu. Towards deep learning models resistant to adversarial attacks. *arXiv preprint arXiv:1706.06083*, 2017. 6
- [34] Tomas Mikolov, Kai Chen, Greg Corrado, and Jeffrey Dean. Efficient estimation of word representations in vector space. *arXiv preprint arXiv:1301.3781*, 2013. 2
- [35] Jesús Andrés Portillo-Quintero, José Carlos Ortiz-Bayliss, and Hugo Terashima-Marín. A straightforward framework for video retrieval using clip. In *Mexican Conference on Pattern Recognition*, pages 3–12. Springer, 2021. 2
- [36] Alec Radford, Karthik Narasimhan, Tim Salimans, Ilya Sutskever, et al. Improving language understanding by generative pre-training. 2018. 2
- [37] Alec Radford, Jong Wook Kim, Chris Hallacy, Aditya Ramesh, Gabriel Goh, Sandhini Agarwal, Girish Sastry, Amanda Askell, Pamela Mishkin, Jack Clark, et al. Learning transferable visual models from natural language supervision. In *International conference on machine learning*, pages 8748–8763. PMLR, 2021. 1, 2
- [38] Chen Sun, Austin Myers, Carl Vondrick, Kevin Murphy, and Cordelia Schmid. Videobert: A joint model for video and language representation learning. In *Proceedings of the IEEE/CVF international conference on computer vision*, pages 7464–7473, 2019. 2
- [39] Hao Tan and Mohit Bansal. Lxmert: Learning cross-modality encoder representations from transformers. *arXiv preprint arXiv:1908.07490*, 2019. 2
- [40] Qiang Wang, Yanhao Zhang, Yun Zheng, Pan Pan, and Xian-Sheng Hua. Disentangled representation learning for text-video retrieval. *arXiv:2203.07111*, 2022. 1, 2, 3, 6, 7, 8, 9
- [41] Wenhao Wu, Haipeng Luo, Bo Fang, Jingdong Wang, and Wanli Ouyang. Cap4video: What can auxiliary captions do for text-video retrieval? In *Proceedings of the IEEE/CVF Conference on Computer Vision and Pattern Recognition (CVPR)*, pages 10704–10713, 2023. 1, 2, 3, 6, 7, 8, 9
- [42] Hu Xu, Gargi Ghosh, Po-Yao Huang, Dmytro Okhonko, Armen Aghajanyan, Florian Metze, Luke Zettlemoyer, and Christoph Feichtenhofer. Videoclip: Contrastive pre-training for zero-shot video-text understanding. *arXiv preprint arXiv:2109.14084*, 2021. 2
- [43] Jun Xu, Tao Mei, Ting Yao, and Yong Rui. Msr-vtt: A large video description dataset for bridging video and language. In *Proceedings of the IEEE conference on computer vision and pattern recognition*, pages 5288–5296, 2016. 1, 2, 3, 6, 7, 8
- [44] Hongwei Xue, Yuchong Sun, Bei Liu, Jianlong Fu, Ruihua Song, Houqiang Li, and Jiebo Luo. Clip-vip: Adapting pre-trained image-text model to video-language representation alignment. *arXiv preprint arXiv:2209.06430*, 2022. 1, 2
- [45] Haozhe Yang, Yuhan Xiang, Ke Sun, Jianlong Hu, and Xianming Lin. Towards video-text retrieval adversarial attack.

- In *ICASSP 2024 - 2024 IEEE International Conference on Acoustics, Speech and Signal Processing (ICASSP)*, pages 6500–6504, 2024. [1](#), [3](#), [6](#)
- [46] Karren Yang, Wan-Yi Lin, Manash Barman, Filipe Condessa, and Zico Kolter. Defending multimodal fusion models against single-source adversaries. In *Proceedings of the IEEE/CVF Conference on Computer Vision and Pattern Recognition*, pages 3340–3349, 2021. [3](#)
 - [47] Ziyi Yin, Muchao Ye, Tianrong Zhang, Tianyu Du, Jinguo Zhu, Han Liu, Jinghui Chen, Ting Wang, and Fenglong Ma. Vllattack: Multimodal adversarial attacks on vision-language tasks via pre-trained models. In *Advances in Neural Information Processing Systems*, pages 52936–52956. Curran Associates, Inc., 2023. [3](#)
 - [48] Zhou Yu, Dejing Xu, Jun Yu, Ting Yu, Zhou Zhao, Yuet-ing Zhuang, and Dacheng Tao. Activitynet-qa: A dataset for understanding complex web videos via question answering. In *Proceedings of the AAAI Conference on Artificial Intelligence*, pages 9127–9134, 2019. [1](#), [2](#), [6](#), [7](#)
 - [49] Jiaming Zhang, Qi Yi, and Jitao Sang. Towards adversarial attack on vision-language pre-training models. In *Proceedings of the 30th ACM International Conference on Multimedia*, page 5005–5013, New York, NY, USA, 2022. Association for Computing Machinery. [2](#), [3](#), [6](#), [7](#), [8](#), [10](#)
 - [50] Jiaming Zhang, Qi Yi, and Jitao Sang. Towards adversarial attack on vision-language pre-training models. In *Proceedings of the 30th ACM International Conference on Multimedia*, page 5005–5013, New York, NY, USA, 2022. Association for Computing Machinery. [3](#)
 - [51] Yunqing Zhao, Tianyu Pang, Chao Du, Xiao Yang, Chongxuan Li, Ngai-Man Cheung, and Min Lin. On evaluating adversarial robustness of large vision-language models. *arXiv preprint arXiv:2305.16934*, 2023. [3](#)
 - [52] Mo Zhou, Le Wang, Zhenxing Niu, Qilin Zhang, Yinghui Xu, Nanning Zheng, and Gang Hua. Practical relative order attack in deep ranking. In *Proceedings of the IEEE/CVF International Conference on Computer Vision*, pages 16413–16422, 2021. [3](#)
 - [53] Linchao Zhu and Yi Yang. Actbert: Learning global-local video-text representations. In *Proceedings of the IEEE/CVF conference on computer vision and pattern recognition*, pages 8746–8755, 2020. [2](#)

Adversarial Video Promotion Against Text-to-Video Retrieval

Supplementary Material

Data Construction. As mentioned in the main paper, we find targeted queries of the ViPro attack by conducting a candidate-wise sortation, as shown in Fig. 9. Specifically, these texts are re-ranked by using them to re-query the model and check the rank of the candidate under these texts. If the candidates are within the top-20 results, the corresponding captions are categorized as targeted queries. The reranked 20 texts are then shuffled and evenly divided into trainsets and testsets. *Re-rank are conducted using the Singularity-17M model.*

Pseudo-code for Temporal Clipping (TC). We provide pseudo-code for Temporal Clipping in Alg.2. TC first calculates the frame-to-frame correlation using cosine similarity to get \mathbf{W}_X , and then calculates the temporal difference between frames $\Delta_{\mathbf{W}_X}$. Frames that exceed γ will be marked as temporally outlying frames and clipped if the clip length is longer than $T/4$, which ensures that the video is not too fragmented to preserve temporal information. We also provide an illustration on the result of TC, as shown in Fig.10.

Categorical Performance. As discussed in the main paper, we use the categorical information provided in [43] and choose the top 10 categories with the best R-Precisions. We provide the R-Precisions for all models on all categories as follows. Interestingly, we find that all categories with low R-Precision are very non-specific words, such as “documentary”, “how-to” and “people”, with which VLMs might find it difficult to relate visual contents. On the other hands, categories with higher precisions are generally ones with concrete implications, such as “animation”, “sports”, and “gaming”. For the distribution of data in each category, please refer to the original paper[43]. Based on the R-Precision, we chose the 10 categories with the highest average performance: Sports, Movie, Animation, Music, Animal, Vehicles, Gaming, News, Education, Cooking.

Algorithm 2 Pseudo-code for Temporal Clipping.

Require: Clean video $\mathbf{X} = [x_1, \dots, x_T]$, video features \mathbf{F}_X
threshold for outlying frames γ
Ensure: Clipped Videos \mathbb{C}

```

1: function TEMPCLIP( $\mathbf{W}_X, \mathbf{X}$ )
2:    $\mathbf{W}_X \leftarrow \text{COSSIM}(\mathbf{F}_X, \mathbf{F}_X)$   $\triangleright T \times T$  temporal similarity
3:    $row \leftarrow 0, \Delta_{\mathbf{W}_X} \leftarrow \text{GETDIFF}(\mathbf{W}_X)$ 
4:   while  $row < T$  do
5:      $col \leftarrow row$ 
6:     while  $col < T$  do
7:        $\Delta \leftarrow \Delta_{\mathbf{W}_X}[row, col]$ 
8:       if  $\Delta \geq \gamma$  then and  $col \geq T/4$ 
9:         Clip the similarity  $\mathbf{W}_X$  and the video  $\mathbf{X}$ 
10:        Break
11:      else
12:         $col \leftarrow col + 1$ 
13:      end if
14:    end while
15:     $row \leftarrow row + 1$ 
16:  end while
17:  return Clipped Videos  $\mathbb{C}$ 
18: end function

```

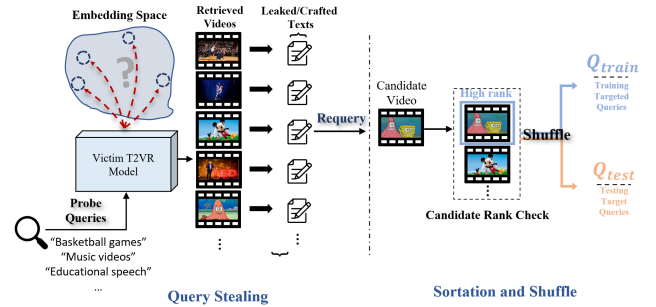


Figure 9. An illustration of data stealing: *i.* Attackers can obtain a diverse subset of training videos and corresponding texts by querying the victim model. *ii.* Attackers can perform a candidate-wise sortation for **each** candidate video by querying the candidate video with the texts from step *i*, checking the rank of the candidate video, and categorizing the texts into **Relevant** and **Irrelevant**.

Table 10. R-Precision for **first 10** categories on all models. The dataset is MSR-VTT-1k. Chosen categories are highlighted in **bold**.

Models	R-Precision (%)									
	Music	People	Gaming	Sports	News	Education	TV shows	Moive	Animation	Vehicles
Sing	35.14	0.00	24.53	42.11	13.79	15.38	20.00	31.15	26.32	25.00
DRL	44.59	0.00	37.74	64.21	29.31	34.62	16.67	49.18	36.84	51.32
C4V	35.14	0.00	35.85	46.32	53.45	42.31	26.67	44.26	57.89	23.68

Table 11. R-Precision for **last 10** categories on all models. The dataset is MSR-VTT-1k. Chosen categories are highlighted in **bold**.

Models	R-Precision (%)									
	How-to	Travel	Science	Animal	Kids	Documentary	Cooking	food	Beauty	Advertisement
Sing	13.04	3.45	11.63	12.07	10.64	0.00	12.50	9.09	11.32	12.50
DRL	13.04	24.14	27.91	55.17	25.53	0.00	37.50	45.45	11.32	16.67
C4V	13.04	31.03	34.88	37.93	8.51	0.00	15.62	33.33	32.08	20.83

Table 12. An ablation study on the influence of the access to the video aggregating transformer within the C4V model. **All attacks have gained a performance boost with access to the aggregator.** Our ViPro maintains its lead in either scenario.

Method	Access to Video Aggregator	R@1(%) ↑	R@5(%) ↑	Average (%) ↑
Co-Attack	X	4.66 (-0.21)	20.86 (-2.08)	12.76 (-1.15)
	✓	26.48 (+22.72)	53.11 (+39.69)	43.05 (+32.21)
SGA	X	0.98 (-3.98)	4.05 (-18.89)	2.52 (-11.39)
	✓	5.20 (+1.44)	18.98 (+5.56)	12.09 (+3.50)
ViPro	X	8.71 (+3.84)	28.9 (+5.85)	18.76 (+4.85)
	✓	77.10 (+73.34)	90.65 (+77.23)	83.88 (+75.29)

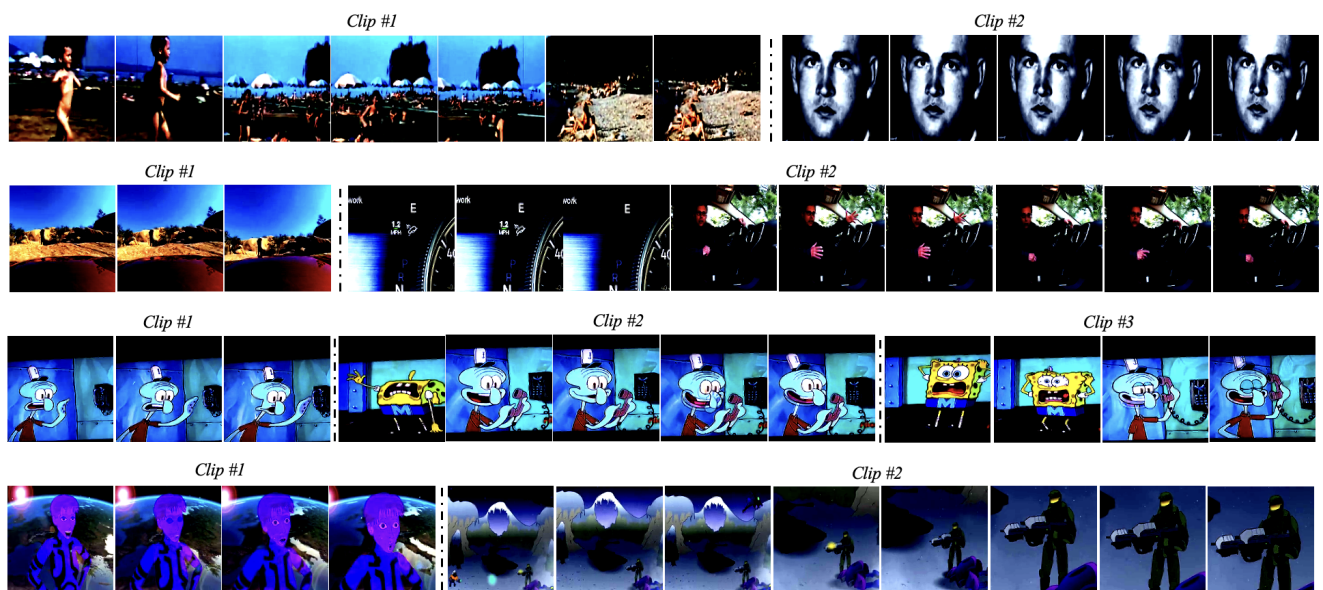


Figure 10. An illustration of the clipped video frames through temporal clipping. All temporally related frames are grouped into clips without creating too fragmented videos, i.e., only 1-2 frames per clip.